ZIBELINE INTERNATIONAL™ PUBLISHING

Water Conservation and Management (WCM)

DOI: http://doi.org/10.26480/wcm.01.2026.249.256

ISSN: 2523-5664 (Print)
ISSN: 2523-5672 (Online)
CODEN: WCMABD

RESEARCH ARTICLE

INTEGRATED HYDROLOGICAL–HYDRAULIC MODELING FOR FLOOD INUNDATION MAPPING AND RISK MANAGEMENT IN DATA-SCARCE ARID WATERSHEDS

Mays Ibrahim Alsaidi [a]*, Ahmed Naseh Ahmed Hamdan[b] and Dina Ali Yaseen[b]

[a]*Dams and Water Resources Engineering Department, Collage of Engineering, Mosul University, Mosul 41002, Iraq*
[b]*Civil Engineering Department, College of Engineering, Basrah University, Basrah, Iraq*
**Corresponding Author Email: mays.ibrahim.alsaidi@uomosul.edu.iq*

Article History:

Received 12 February 2026
Revised 20 March 2026
Accepted 14 April 2026
Available online 19 May 2026

ABSTRACT

Southern Iraq, especially Wasit and Maysan governorates, is experiencing flash flooding and water shortages. Limited hydrological research and streamflow data limit runoff estimates, flood risk assessment, disaster preparation, and floodwater harvesting. Simulating the hydrological and hydraulic response of a 2,945.33 km^2 watershed during a March-May 2019 flood and modelling rainfall-runoff processes with 2019 daily rainfall data in ArcGIS, HEC-HMS, and 2D HEC-RAS highlights the potential for floodwater harvesting to address seasonal shortages. In the HEC-HMS software, the SCS-CN method for losses, the SCS Unit Hydrograph for transformation, and the Muskingum routing method were used to compute run-off in each watershed reach. The extracted discharge outputs were input as upstream boundary conditions to a 2D HEC-RAS model to estimate flood extent. Simulations revealed about 144.4 million m^3 of runoff volume, with initial abstraction (Ia) having the greatest impact on volume. Qualitative comparison with Sentinel-2 satellite imagery from a similar flood occurrence indicated good spatial consistency for model validation. Because of their concentration on flood forecast accuracy, quantitative measures like CSI were evaluated but not employed as validation evidence. Although data is rare in ungauged arid basins, integrated modelling can improve water planning and flood risk management if monitored and regulated.

KEYWORDS

Rainfall-Runoff Modelling; Risk Management; Flood Simulation; Hydraulic Modelling; HEC-HMS/HEC-RAS.

1. INTRODUCTION

Iraq faces a perplexing water crisis characterized by frequent flash floods and prolonged droughts. In regions such as southeastern Iraq, where temperatures are rising and rainfall is decreasing, there is a greater need for accurate hydrological information (Noma and Mohammed, 2017). This endangers infrastructure, ecosystems, and human lives. In March 2019, floods in southern Iraq, particularly in the northern Maysan Governorate, compelled over 170,000 individuals to evacuate their residences and inundated more than 100 villages (IOM, 2022). This highlights the importance of integrated water risk management systems that can utilize floodwater during rare storms and contribute to addressing long-term water shortages induced by climate change and the construction of dams upstream (Al-Muqdadi, 2019).

Integrated, data-driven frameworks that are becoming more and more significant in current hydrological modelling include GIS, remote sensing, and physics-based simulation tools. DEMs are utilized as basic inputs to get watershed features, including drainage networks, slope, and flow direction, which are very important for modelling runoff and floods (Maidment, 2002; Shamsi, 2008).

The analysis made a high-resolution CN map for the Lesser Zab watershed using GIS, HEC-GeoHMS, and remote sensing. This map is very important for HEC-HMS-based runoff simulations in ungauged basins (Salman and Hamdan, 2023). It also lets you accurately estimate the flood volumes that can be harvested, which is an important step in figuring out how much water can be harvested before hydraulic modelling. The study provide further context by demonstrating that machine learning (Random Forest) achieves 84.7% accuracy in Hydrologic Soil Group (HSG) classification, markedly surpassing traditional methods (54%), thereby facilitating more reliable CN assignment (Abraham et al., 2019).

The main focus of the research is on several sub-watersheds that straddle the border between Ilam Province, Iran, and Ali Al-Gharbi, Iraq. These areas are very different from one another (Ali et al., 2023). In northern Iran, there are high, semi-arid mountains, and in southern Iraq, there are flat, very dry lands. This paper used GIS and remote sensing to look at how dangerous soil erosion will be from 2017 to 2020. The results show that erosion is quite rare in the Iraqi lowlands, with only the steep, high-rainfall slopes of the Iranian uplands showing significant erosion. This shows that flooding in southern Iraq (like in Maysan) is mostly caused by low infiltration and poor drainage on flat land, not by sediment transport or soil loss in the uplands.

Developed a complete take-in from the flood strategy for the Diyala River Basin using HEC-HMS and 2D HEC-RAS. Their method made a clear connection between hydrological modelling and water harvesting: HEC-HMS created runoff hydrographs using the SCS-CN methodology, and these discharge outputs were input as upstream boundary conditions to a 2D HEC-RAS model to simulate spatial inundation (Alrammahi and Hamdan, 2014). The model, which was calibrated using satellite images

Quick Response Code	Access this article online	
	Website: www.watconman.org	DOI: 10.26480/wcm.01.2026.249.156

Cite The Article: Mays Ibrahim Alsaidi, Ahmed Naseh Ahmed Hamdan and Dina Ali Yaseen (2026). Integrated Hydrological–Hydraulic Modeling For Flood Inundation Mapping and Risk Management in Data-Scarce Arid Watersheds. Water Conservation and Management, 10(1): 249-256.

from 2019, detected recurrent flood maxima in March and April, with water levels at Hemrin Dam surpassing 110 meters (crest level: 109.5 meters). In order to mitigate this, the authors suggested building an artificial diversion canal that would direct up to 1.24 billion m^3 of floodwater to Al-Shweijah Marsh. During summer droughts, this water could be diverted to the Tigris River, turning flood risk into a valuable water resource for groundwater recharge, irrigation, and salinity control.

Analysis used a 1D/2D HEC-RAS model to investigate how a proposed regulator might impact floods on the Shatt Al-Arab River (Hamdan et al., 2019). Their research validated the two-dimensional hydraulic model for flood mapping using a simulated flood wave of 200 m^3/s; however, they did not utilize HEC-HMS software due to data limitations. There were discharge gauge stations, which were used as boundary conditions for the hydraulic model (HEC-RAS). The authors used different scenarios to regulate the gates of the regulator. The authors suggested the creation of lateral canals and the elevation of riverbanks to facilitate the controlled collection of floodwaters for advantageous use during dry spells.

New evidence suggests that a solution to Iraq's two water problems can be found by combining integrated hydrological and hydraulic models with high-resolution DEM and dynamic land use data (HEC-HMS and 2D HEC-RAS). This technology enables the protection of low-lying areas in northern Maysan, near the Tigris River, and the accurate identification of flood-harvesting sites. This study is noteworthy because it is the first of its kind to apply an integrated hydrological-hydraulic framework to the Ali al-Gharbi watershed. The study relies on the CN values extracted for the same area as input to the HEC-HMS model for surface runoff simulation by (Alsaidi et al., 2025). The hydrograph outputs are then transferred to the 2D HEC-RAS model to generate accurate flood inundation maps for the November 2019 event. The maps are then qualitatively verified via satellite imagery due to the scarcity of measured discharge data. This allows for the estimation of hydraulic parameters in unmeasured areas and encourages effective water management strategies, such as collecting seasonal floodwater for reuse during drought and improving the area's abilities. Therefore, the main knowledge gap lies in the lack of application of integrated modelling (HEC-HMS/HEC-RAS) and quantitative spatial validation in an understudied semi-arid watershed in southern Iraq, and this study is the first attempt to fill this gap.

2. Materials And Methods

2.1 Study Area

The study was conducted in southern Iraq, between 32°00' and 32°38' north and 46°00' and 46°45' east (Figure 1). The basin is surrounded by the southern Iraqi governorates of Wasit and Maysan. The basin is approximately 505.84 km long and has a total area of 2945.33 km^2. The region is an ungauged basin, lacking river discharge data, and thus requires dependence on indirect hydrological modelling and remote sensing methods.

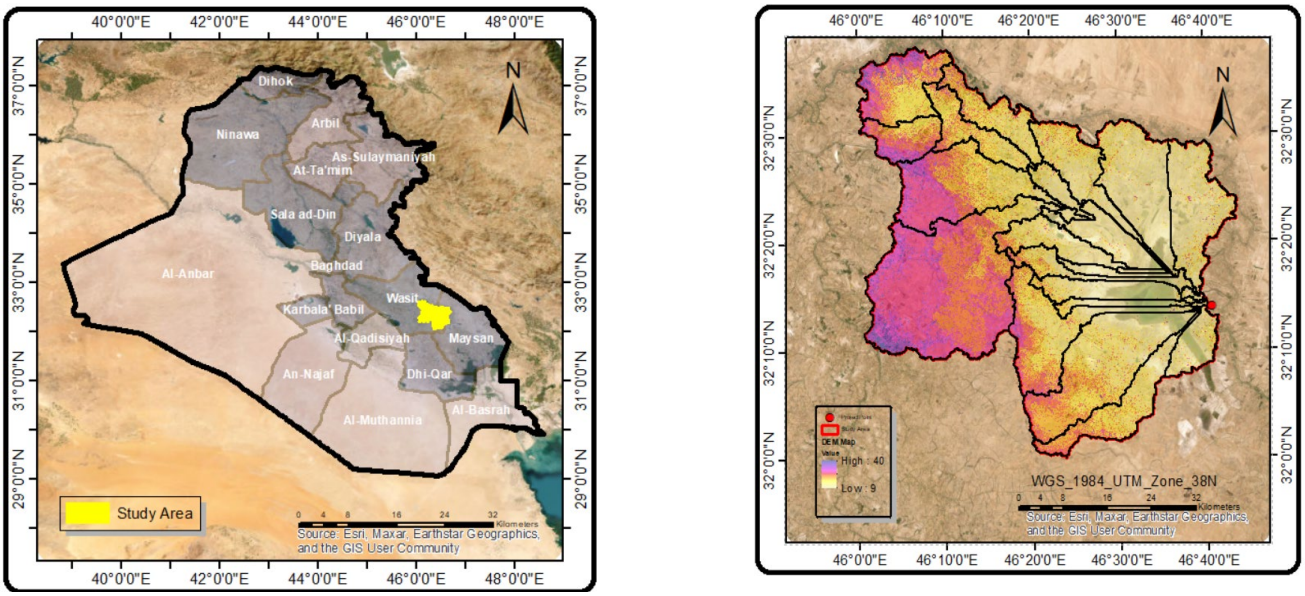

(a) Study Area

(b) Watershed Subbasins

Figure 1: Layout of the watershed, a) Study Area, b) Watershed Subbasins

2.2 Data Sources

Table 1 presents statistics on land usage, soil type, geography, and rainfall data, along with the data sources for each. Table 1 shows the extensive collection of geographical and hydrological data used in this investigation. For this purpose, we used the findings of the study conducted on this specific watershed by (Alsaidi et al., 2025). The study accurately determined the distribution of the CN index in terms of region. Soil CN values, land use data, and the DEM were the primary inputs to the HEC-HMS model in this study, which relied on the basic hydrological parameters supplied by the prior study.

Dry to semi-arid environments prevail in the Maysan Governorate. According to the Iraqi Ministry of Water Resources, the study region has an average annual rainfall of 103 mm. The average daily temperature in March-May 2019 was 22.5°C, which is consistent with usual spring temperatures in the region (IAC, 2026).

Table 1: lists the Rainfall Runoff Model's input data as well as the source from which it was abstracted

Data	Data source
SRTM (Shuttle Radar Topography Mission)/ SRTM 1 Arc-Second Global/High-resolution data (30 meters)	United States Geological Survey (USGS) National map viewer. Website: https://earthexplorer.usgs.gov/
Land use data 2019	ESRI data from 2019–2020, 10 m resolution https://livingatlas.arcgis.com/landcoverexplorer/#mapCenter
Soil type Data	FAO Global Soil Grid. https://www.fao.org/soils-portal/data-hub/soil-maps-and-databases/harmonized-world-soil-database-v12/en
Rainfall, Runoff, Gage Height data	Ministry of Agriculture, Iraqi Agrometeorological Center, https://www.agromet.gov.iq/

2.3 HEC-HMS Model Setup and Configuration

The HEC-HMS is a physically based, semi-distributed modelling platform designed to simulate rainfall–runoff processes in dendritic watershed systems. By connecting important components, subbasins, reaches, junctions, and diversions into a structured downstream network, where flow originates from upstream components and flows towards the outlet, the model depicts hydrologic response (Ihimekpen and Ilaboya, 2018). It is widely used in flood predictions, reservoir management, and stream restoration studies.

For this study, the watershed was divided into multiple sub-basins using a three-month precipitation record, whereas HEC-HMS employs recorded precipitation statistics to simulate the conversion of rainfall into runoff within a watershed (Halwatura and Najim, 2013). The SCS Unit Hydrograph method was used to convert surplus rainfall into direct runoff, the Muskingum methodology was used for channel routing, and the CN approach was used to estimate rainfall losses in accordance with the HEC-HMS user's manual (2000) (Hameed et al., 2019).

2.3.1 Estimating Parameters

- Loss Model

Direct runoff from a design storm was predicted using the SCS-CN method. This approach is well recognized for its simplicity, robustness, and consistent outcomes when assessing precipitation excess based on cumulative rainfall, land cover, soil type, and antecedent moisture conditions (Hamdan et al., 2021, Herbei et al., 2024). The following equation is used to Fig. out the amount of extra rainfall (P_e):

$$P_e = \frac{(P-I_a)^2}{P-I_a+S} \qquad \text{for } P>Ia \tag{1}$$

To find the extra rain that fell during a certain time period, you have to subtract the total amount of additional rain that fell from the beginning of that period to the end. One important part of this scheme is the dimensionless CN. It links the retention measure S to factors such as the hydrologic soil type, the land's use or treatment, and the amount of water present before. Here's how to describe the connection between CN and S:

$$S = \frac{25400-254CN}{CN} \tag{2}$$

With this method, the land and soil's physical features can be turned into a number score that shows how probable it is to produce flow.

- Transform Model

In order to simulate the transformation of surplus precipitation into direct runoff, this research utilises the SCS unit hydrograph method. The technique is based on a one-peak generic, dimensionless hydrograph that represents the runoff response of the watershed over time. The time difference between the effective rainfall's centre of mass and the accompanying hydrograph peak is represented by the lag time (T_{lag}), an important quantity in this formulation. The following equation (Salami et al., 2017) is used to experimentally link T lag to the time of concentration (T c), in accordance with accepted technical guidance:

$$T_{lag} = 0.6Tc \tag{3}$$

The two variables utilise minutes as their unit of measure.

The time of concentration, which is the time it takes for runoff to flow from the catchment's hydraulically most distant point to the outlet, was computed using Kirpich's empirical formula from 1940. This equation was chosen because it works well in small to medium-sized catchments and is often used in watersheds that don't have a lot of data. The method depends exclusively on easily accessible morphological characteristics (i.e., flow length and channel slope) that can be precisely extracted from DEM, making it especially appropriate for areas with limited hydrological data. Additionally, Kirpich's equation has been effectively utilised in many dry and semi-arid areas, providing commendable accuracy for flood estimation in data-scarce scenarios. The equation is expressed as:

$$T_C = 0.0078 \, . L^{0.77} . S^{-0.385} \tag{4}$$

The average slope of the watershed is shown by S, which is found by dividing the total drop in elevation along the main flow channel by its length. L is the length of the longest flow route, expressed in metres. This approach enables a practical and widely accepted calculation of Tc based on measurable basin parameters.

- Routing Model

The dynamic development of flow over river reaches is modelled using the Muskingum routing technique, which is based on simplified versions of the continuity and momentum equations. The Muskingum method was selected due to its minimal data requirements and computational efficiency, making it particularly suitable for data-scarce regions where detailed cross-sectional information is limited (Reddy, 2005). According to this method, channel storage is made up of two parts: a wedge that changes with intake and outflow, and a prism with a fixed cross-section. The continuity equation's finite difference approximation is written as follows

$$\left(\frac{I_{t-1}+I_t}{2}\right) - \left(\frac{O_{t-1}+O_t}{2}\right) = \left(\frac{S_t-S_{t-1}}{\Delta t}\right) \tag{5}$$

In this expression, the storage volumes in the reach at the start and finish of the time step are represented by S_{t-1} and S_t, the associated outflows by O_{t-1} and O_t, and the inflows by I_{t-1} and It. The symbol for the time step is Δt.

The Muskingum model further defines storage at time t as a weighted combination of inflow and outflow:

$$S_t = KQ_t + KX(I_t - Q_t) = K[XI_t + (1-X)Q_t] \tag{6}$$

In this case, X is a dimensionless weighting factor that typically ranges from 0 to 0.5, and K is the storage time constant (in time units). Prism storage is denoted by the word KQ_t, whereas the wedge storage component is denoted by KX ($I_t - Q_t$).

In this study, the HEC-HMS hydrologic modelling platform was used to simulate rainfall-runoff processes for the branching catchment system. Spatial and temporal information, among other input data needed by HEC-HMS, was extracted from GIS-based feature databases and applied, either automatically or manually, to specific sub-basins and river reaches. Among the important parameters assigned were: Loss parameters: percentage of impervious area (Ia), and CN; Transform parameters: unit hydrograph generation lag time; Muskingum coefficients K and X are the routing parameters (HEC-HMS Technical Reference Manual, 2013).

Furthermore, paired data on sub-basin hypsometry were used to establish an elevation–area relationship. The Time Series Data Manager was used to import meteorological inputs as time series. In order to provide rainfall data for the control simulation, three meteorological files were created. All hydrograph calculations were performed using a daily time step, and the modelled wet season run from March 1 to May 31.

2.4 HEC-RAS Setup and Parameterization

The two-dimensional unsteady flow capabilities of HEC-RAS were used to simulate the hydraulic behavior of the study area, enabling a thorough evaluation of the evolution of flood depths under dynamic conditions (Lenka, 2019). The model configuration included three key datasets: simulation control settings (plan data), flow inputs, and a morphological representation of the river system. River reaches and sub-basins were among the geometric boundaries that were imported as shapefiles from HEC-HMS. An appropriate Manning's n value was assigned throughout the floodplain using a land cover map (Table 1) and added to the model as a GeoTIFF raster layer using RAS Mapper to account for spatial variability in surface roughness. A normal depth assumption was used at the downstream boundary, whereas discharge hydrographs produced by HEC-HMS for each tributary feeding the system served as the basis for the upstream boundary conditions. The terrain-processing tools of RAS Mapper were used to automatically create bank stations and cross-sections in HEC-RAS. The extent and level of floodwaters during the simulation period were then clearly visualized by creating high-resolution inundation maps using the same environment.

2.5 Sensitivity analysis

A parameter influence assessment was conducted to examine how adjustments to key inputs in the HEC-HMS watershed modelling framework affect simulated hydrologic responses across the study basin, outputs that subsequently served as boundary conditions for the hydraulic simulations in HEC-RAS. Given the scarcity of in situ precipitation and streamflow measurements, baseline parameter values were refined incrementally, guided by ranges reported in peer-reviewed studies and analogous catchment analyses.

Due to a lack of field or real-world data, the sensitivity analysis of the hydrological process model did not include CN curve values, which are established methods (ESRI 2019 LULC, HWSD soil data, and USDA-SCS classification). CN values were generated from the GIS created by Alsaidi et al. (2025) for the Ali Al-Gharbi watershed. In areas ungauged or with insufficient stations, these established parameters conform to best practices in hydrological modeling.

The percentage of impervious surfaces is a key indicator of urbanization and built-up areas, and sensitivity analysis of this parameter reveals the

influence of urbanization on the watershed's hydrology. Initial infiltration (Ia) refers to the soil water content before runoff, and sensitivity analysis of Ia shows how soil type and land use influence infiltration and surface runoff. The K and X parameters of the Maskingum method of the river determine the water travel time within its channel, and sensitivity analysis of these parameters reveals how the river's characteristics influence its hydrological response.

This sensitivity-based diagnostic approach helped determine which inputs were most important for the model's response and, by ranking them, improved the trustworthiness of the simulation findings.

2.6 Model Calibration and Validation

In fact, split-sample testing, which divides data into subsets for calibration, validation, and occasionally testing, is currently recommended by best practices in order to guarantee reliable model evaluation (Najafi et al., 2024). According to (Yeh and Chen, 2022)"validation is not a formality, it is the ultimate test of whether a model genuinely understands the system or only memorizes the calibration period."

Calibration frequently uses sensitivity analysis to find and modify important parameters until simulated outputs match remotely detected flood patterns due to the lack of reliable hydrological data, exemplified by the absence of discharge gauges at specific points within the watershed (Domeneghetti et al., 2021). This integration is frequently the only practical method for reliable flood modeling in ungauged catchments, as noted by (Sayama et al., 2025). To measure the geographical agreement between predicted and observed inundation, this performance evaluation method has been frequently used in recent flood modeling research.

The hydrological and remote sensing groups advocate using the Critical Success Index (CSI), Hit Rate (HR), and False Alarm Ratio (FAR) as standard categorical metrics to validate flood extent estimates (Eilander et al., 2025, Yousif, and Hamdan, 2026). The satellite-derived inundation map and the simulated HEC-RAS 2D flood extent were first transformed from vector polygons to raster layers and classed in ArcGIS, with water pixels given a value of 255 and non-water pixels a value of 0, in order to calculate the CSI. Equation (7) was applied once the two binary rasters were superimposed using the Raster Calculator tool:

$$CSI = \frac{Smod \cap Sobs}{Smod \cup Sobs} \times 100 \quad (7)$$

where S_{mod} is the area that the model projected would be flooded, and Sobs is the area that was discovered to be inundated in the satellite image. The CSI ranges from 0% to 100%, with 100% representing perfect spatial correlation. Furthermore, HR and FAR were calculated using Equations (8) and (9), respectively, to assess potential model bias toward under- or over-prediction (Zotou et al., 2022):

$$HR = \frac{Smod \cap Sobs}{Sobs} \times 100 \quad (8)$$

$$FAR = \frac{Smod - (Smod \cap Sobs)}{Smod} \times 100 \quad (9)$$

Both indices have a range of 0 to 100%. The HR shows the proportion of satellite-inundated areas that the model also projected would flood; a value of 100 means that the model expected all satellite-inundated areas would flood. On the other hand, the FAR shows if the model overestimates the flood's size; values of 0 and 100% denote the absence of false alarms and the presence of all false alarms, respectively.

3. Results

3.1 Utilizing ArcGIS output for HEC-HMS modelling

Alsaidi et al. (2025) spatially distributed basin CN values from 71 to 100 using an integrated geoprocessing approach. Most of the watershed (94.05%) is agricultural land with low runoff (CN = 77). However, open water bodies, which account for 2.64% of the basin, were given a CN value of 100 to signify run-off. Urban and residential zones had higher CNs (91–100) because of their high imperviousness and low infiltration capability. The HEC-HMS modelling system relies on this thematic layer to estimate peak discharge and transform rainfall-runoff. After its implementation, flood estimates in the study area are more accurate and realistic (Belina et al. 2024; Fanta and Tadesse 2022).

This research develops a core prediction system hydrologic model designed to evaluate flood scenarios and estimate regional runoff magnitudes. As seen in Fig.2 estimated hydrograph of the watershed outflow, Table 2 shows peak flows between March and May 2019, the region's principal flood season. The depth and amount of flow were rising, making floods more likely. As of April 2, 2019, the model forecast a maximum volume of 144.4 million m^3 at outlet 1.

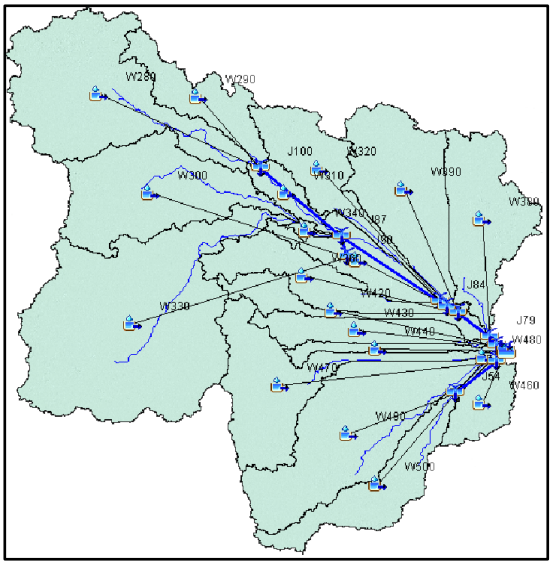

Figure 2: Hydrologic modelling system for the watershed at HEC-HMS

Table 2: Details of the model

Sub Basin	Area (km^2)	CN	Lag Time (min)	Volume (1000 m^3)
W280	328.714	83.410	1191.973	15395.7
W290	101.412	80.754	1135.309	6664.9
W300	252.785	85.956	1055.965	10752
W310	38.013	86.155	690.033	28.4
W320	129.844	83.195	884.837	28586.5
W330	562.036	85.927	1348.384	12896.5
W340	7.66	85.933	609.570	15065

Table 2(Cont.): Details of the model				
W350	90.296	85.255	805.084	4144.8
W360	123.35	85.942	875.821	1951.4
W380	190.717	81.647	671.213	389.7
W390	220.791	82.478	973.779	4477.3
W420	68.619	86.342	732.474	5911.2
W430	87.471	89.451	705.781	9725.7
W440	33.255	90.113	591.114	6277.7
W450	0.048	79.000	16.467	8105.3
W460	66.284	85.767	340.686	5117.2
W470	204.916	86.653	754.947	3555.8
W480	0.556	86.000	156.223	3349.4
W490	303.069	85.895	749.355	1995.9
W500	135.495	85.059	790.988	1.8
Outlet1	2945.33			144.4

3.2 Sensitivity Analysis

The model's sensitivity was judged by: the impervious percentage, the initial abstraction (Ia), and Muskingum K and X. This sensitivity analysis did not include CN values, which were consistent with those utilized in the previous HEC-GeoHMS setup (see Figure 3). Varying a single parameter and keeping all other parameters constant, and verifying the variations of outputs. The model output of default values was maintained as the benchmark, and the subsequent outputs of the model of any change in any parameter were compared with the base. The analysis consisted of the range of +50 to -50 with ±10 steps each.

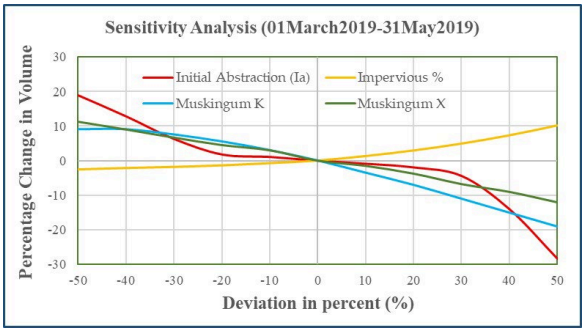

Figure 3: Sensitivity Analysis

The sensitivity analysis shows that Initial Abstraction (Ia) is the most important factor. It can affect the volume of runoff by ±19–30% when it changes by ±50%, which is because it is so important for influencing when runoff initiates in arid watersheds. Muskingum K came in second, with an inverse relationship (around 19% change), which shows how it affected channel storage and flow attenuation. On the other hand, the impervious percentage revealed very little sensitivity (<10%), which means that the default land cover values are good enough to represent the watershed. These results show how important it is to prioritize the calibration of Ia and K while avoiding over-parameterization of less sensitive variables. This will make the model more efficient and reliable for predicting floods in dry areas where there is not enough information.

3.3 HEC-RAS Modelling

The hydraulic simulation employed a flow hydrograph as a boundary condition and unsteady flow conditions between March 1 and May 31, 2019. This process began with the production of the DEM in RAS Mapper, where river reaches and cross-sections were identified to ensure an accurate depiction of channel geometry (see Figure 4). The accurate calculation of flood depths throughout the research region was made possible by the collection of elevation data at each cross-section. A two-dimensional (2D) modelling approach was used for this, and the computerized grid size was selected to strike a balance between accuracy and response time. Although a smaller grid size increases the model's accuracy, it requires more computation time without changing the amount of flooding (see Figure 5).

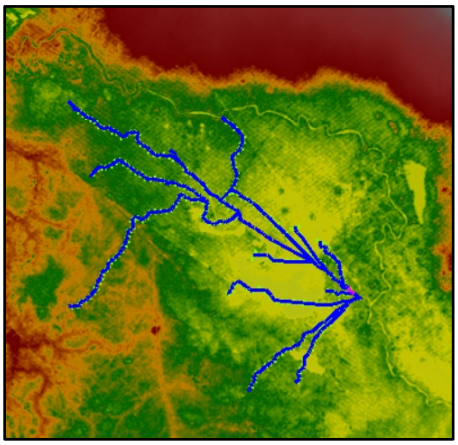

Figure 4: Created the Ras Mapper terrain, river reaches, and cross sections

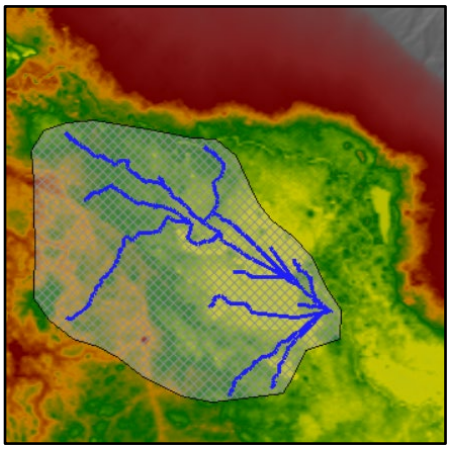

Figure 5: Created the polygon and Mesh size in the study area

3.3.1 Manning Roughness Coefficient

In two steps, Manning's values, which are crucial for the hydraulic model, were computed and input into Ras Mapper. First, as seen in Figure 6, a land cover image was downloaded from the NASA website and applied to Ras Mapper as a layer. As seen in Figure 7, the second stage was to add Manning coefficient values to each type of land in a necessary table.

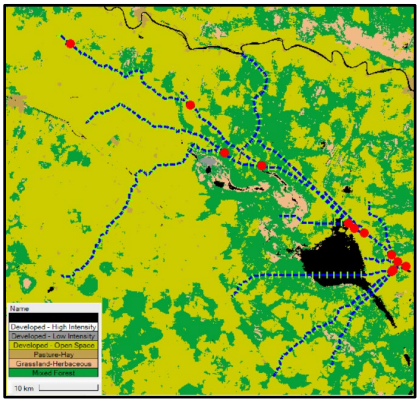

Figure 6: Manning's Roughness Layer

Classification Parameters

ID	Name	ManningsN
0	NoData	0.15
11	Mixed Forest	0.2
5	Developed - Open Space	0.15
8	Grassland-Herbaceous	0.24
7	Pasture-Hay	0.28
1	Unclassified	0.15
2	Developed - High Intensity	0.13
4	Developed - Low Intensity	0.04

Figure 7: Manning's Roughness Values

3.3.2 Model Calibration and Validation

The CSI was used to compare the flood map findings with the real satellite image taken on April 2, 2019 (https://earthmap.org/compare.html?geoJson/), as shown in Figure 8 (Sadana et al., 2025). The result of CSI was 82.43%, HR was 93.89%, and FAR was 12.89%. A study by Yousif and Hamdan (2026) used the configuration similarity index (CSI) to evaluate the results of HEC-RAS simulations against flood maps extracted from satellite imagery. The results showed that the tested model performed well under real-world conditions, with a calibrated CSI of 78.56% and a validated CSI of 82.56%.

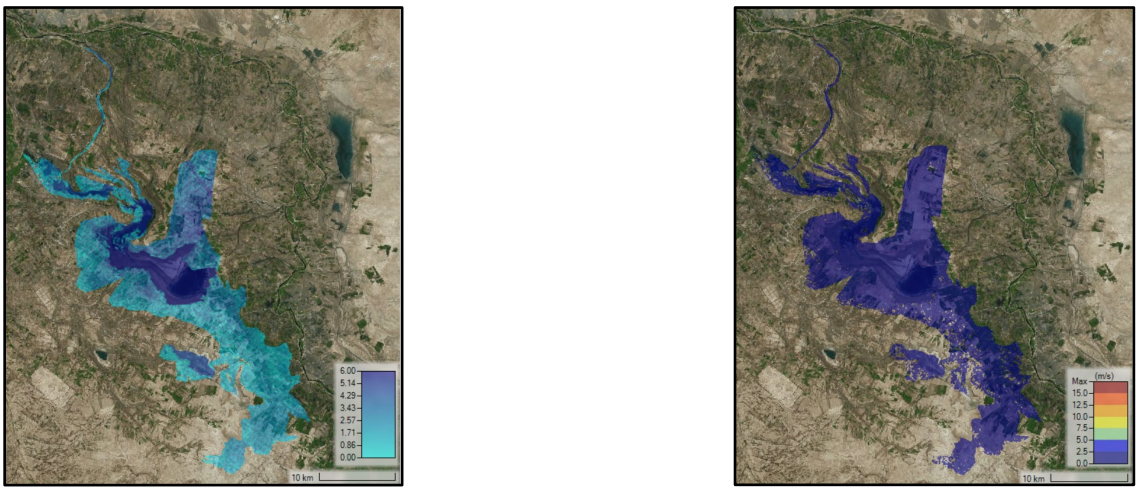

(1) (2)

(a)

(b)

Figure 8: (a.1): hydraulic modelling of flood water depth using HEC-RAS, **(a.2):** velocity of floodwater map **(b)**: actual satellite image at the same time (April 2, 2019)

The model was validated by including these verified and corrected parameters in the flood that happened on November 27, 2018(https://earthobservatory.nasa.gov/images/144308/floods-swamp-iraq) as shown in Figure 9, and guaranteeing the model's dependability after the calibration steps were completed by altering some of the most sensitive hydrological parameters in accordance with the aforementioned sensitivity analysis and attaining the precise convergence between the simulation and reality. It was found that the April 2, 2018, flood event had CSI = 89.0%, HR = 98.2%, and FAR = 9.5% when simulated and satellite-derived flooding were compared.

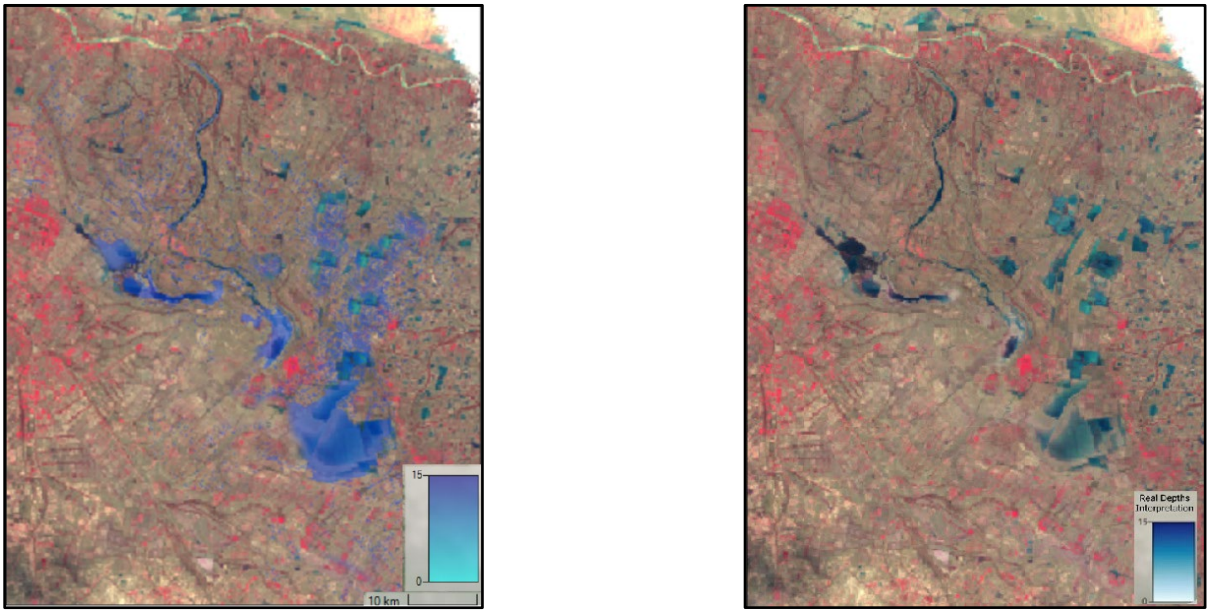

(a) (b)

Figure 9: a) Hydraulic modelling flood water depth using HEC-RAS, 2D, **b:** actual satellite image at the same time (November 27, 2018)

4. Discussion

By using the amount of rain that fell as input in HEC-HMS, the simulation results showed a significant amount of runoff over the modeled period, with approximately 144.4 million cubic meters (Mm^3) of runoff from the surface and a high release of 489.7 m^3/s on April 2, 2019. However, this method of checking the model was limited because it wasn't possible to directly compare simulated and real flows, as there was no measurable streamflow data available at the outlet. With the region's frequent droughts and ongoing water scarcity, this amount might be seen as both a flood risk and a valuable strategic asset. The quantitative calibration indices obtained in this study (CSI = 82.43%, HR = 93.89%, FAR = 12.89%) indicate that the model works satisfactorily to predict the extent of flooding in semi-arid watersheds without hydrological stations. Comparing these studies to regional ones reveals that they usually employed discharge-based calibration with gauge data, and that these studies have mostly concentrated on northern gauged basins or big rivers like the Tigris and the Euphrates. Also, for spatial validation, quantitative spatial metrics (CSI, HR, FAR) are recommended for ungauged basin assessment. In validation on November 27, 2018, it was found that the flood event had CSI = 89.0%, HR = 98.2%, and FAR = 9.5% when simulated and satellite-derived flooding were compared. These are qualities that are especially helpful in places with limited data, where accurate flood risk assessment is hard to do but very important. The CSI had some small problems that weren't caused by major problems with the model itself. Instead, they were caused by outside factors, mostly the spatial resolution of the DEM and some unrealistic assumptions built into the HEC-HMS hydrologic routines. In conclusion, the calibrated and confirmed model does a great job of simulating how floods move across the study area.

5. Conclusions And Recommendations

Flood risk management requires geospatial risk analytics and accurate meteorological predictions, the study found. Durable infrastructure requires several years of rainfall estimates and 50–100-year return periods. Hydrological models like HEC-HMS simulate surface water flow, and 2D hydraulic simulations like HEC-RAS predict flood spread. AI and machine learning boost long-term forecasting in this modeling chain. Community early warning and scenario-based evacuation preparation are simplified. practical floodwater harvesting infrastructure, with specific recommendations for (1) concrete-lined conveyance channels with radial gate terminals, (2) small earthen check dams for runoff control, (3) off-channel retention ponds for irrigation storage, (4) infiltration basins for groundwater recharge, and (5) integration with existing irrigation networks. Design parameters (dimensions, materials, capacities) are provided based on modeled peak discharge and runoff volumes. Flood models must be validated against real-time meteorological, remote sensing, and hydrological records for long-term success. A complete flood inventory and adaptive basin management in data-poor areas would result.

Declarations

Data Availability

The data shall be made available upon request.

Competing Interests

The authors declare that they have no competing interests.

Funding

Not Applicable.

Authors' Contributions

The authors confirm their contribution to the paper. All authors reviewed the results and approved the final version of the manuscript.

Acknowledgements

The authors gratefully acknowledge the support provided by the Iraqi Agrometeorological Center, Ministry of Agriculture, which contributed to the provision of data, and also to the Civil Engineering Department, Faculty of Engineering, Basrah University.

References

Abraham, S., Huynh, C., and Vu, H., 2019. Classification of soils into hydrologic groups using machine learning. Data, 5(1), 2. https://doi.org/10.3390/data5010002

Ali, A.A., Al-Abbadi, A.M., Jabbar, F.K., Alzahrani, H. and Hamad, S., 2023. Predicting soil erosion rate at transboundary sub-watersheds in Ali Al-Gharbi, southern Iraq, using RUSLE-based GIS model. Sustainability, 15(3), Pp. 1776. https://doi.org/10.3390/su15031776

Al-Muqdadi, S.W., 2019. Developing strategy for water conflict management and transformation at Euphrates–Tigris basin. Water, 11(10), 2037. https://doi.org/10.3390/w11102037

Alrammahi, F.S., and Ahmed Hamdan, A.N., 2024. Hydraulic model for flood inundation in Diyala River Basin using HEC-RAS, PMP, and neural network. Open Engineering, 14(1), 20220530. https://doi.org/10.1515/eng-2022-0530

Alsaidi, M. I., Hamdan, A. N. A., and Yaseen, D. A., 2025. Runoff Modeling

Using the GIS-Based Curve Number Method. The Eurasia Proceedings of Science, Technology, Engineering and Mathematics (EPSTEM), 37, Pp. 754-764. https://faculty.uobasrah.edu.iq/uploads/publications/1770413351.pdf

Belina, Y., Kebede, A., and Masinde, M., 2024. Comparative analysis of HEC-HMS and machine learning models for rainfall-runoff prediction in the upper Baro watershed, Ethiopia. Hydrology Research, 55(2), Pp. 432–449. https://doi.org/10.2166/nh.2024.023

Domeneghetti, A., Molari, G., Tourian, M.J., Tarpanelli, A., Behnia, S., Moramarco, T., and Brath, A., 2021. Testing the use of single- and multi-mission satellite altimetry for the calibration of hydraulic models. Advances in Water Resources, 151, 103887. https://doi.org/10.1016/j.advwatres.2021.103887

Eilander, D., Couasnon, A., Leijnse, T., Ikeuchi, H., Yamazaki, D., Muis, S., and Ward, P.J., 2023. A globally applicable framework for compound flood hazard modeling. Natural Hazards and Earth System Sciences, 23(2), Pp. 823–846. https://doi.org/10.5194/nhess-23-823-2023

Fanta, S.S. and Tadesse, S.T., 2022. Application of HEC–HMS for runoff simulation of Gojeb Watershed, southwest Ethiopia. Modeling Earth Systems and Environment, 8(2), Pp. 1327–1342. https://doi.org/10.1007/s40808-021-01337-5

Halwatura, D. and Najim, M.M.M., 2013. Application of the HEC-HMS model for runoff simulation in a tropical catchment. Environmental Modelling & Software, 46, Pp. 155–162. https://doi.org/10.1016/j.envsoft.2013.03.006

Hamdan, A.N.A., Abbas, A.A. and Najm, A.T., 2019. Flood hazard analysis of proposed regulator on Shatt Al-Arab River. Hydrology, 6(3), 80. https://doi.org/10.3390/hydrology6030080

Hamdan, A.N.A., Almuktar, S. and Scholz, M., 2021. Rainfall-runoff modeling using the HEC-HMS model for the Al-Adhaim River catchment, northern Iraq. Hydrology, 8(4), 178. https://doi.org/10.3390/hydrology8040178

Hameed, H.M., Faqe, G.R. and Rasul, A., 2019. Effects of land cover change on surface runoff using GIS and remote sensing: A case study Duhok sub-basin. In: Environmental Remote Sensing and GIS in Iraq. Springer International Publishing, Pp. 205–223. https://doi.org/10.1007/978-3-030-21344-2_9

Herbei, M.V., Bădăluță-Minda, C.A., Popescu, C., and Pătru-Stupariu, I., 2024. Rainfall-runoff modeling based on HEC-HMS model: A case study in an area with increased groundwater discharge potential. Frontiers in Water, 6, 1293389. https://doi.org/10.3389/frwa.2024.1293389

Hydrologic Engineering Center, 2013. HEC-HMS quick start guide. US Army Corps of Engineers.

Ihimekpen, N.I., and Ilaboya, I.R., 2018. Assessment of rainfall-runoff relations for sustainable water resources management in Ethiope watershed using SCS-CN, ARC-GIS, ARC-HYDRO, HEC-GEOHMS and HEC-HMS. Trends in Civil Engineering and Its Applications, 2(1), Pp. 1–7.

International Organization for Migration (IOM), 2022. Migration, environment, and climate change in Iraq. International Organization for Migration. https://www.iom.int/

Lenka, B., 2019. Rainfall-runoff estimation of Ong River basin using SCS-CN method in HEC-HMS with the help of GIS and remote sensing. International Journal of Advanced Engineering Research and Science, 6(12), Pp. 45–54.

Maidment, D.R. (Ed.), 2002. Arc Hydro: GIS for water resources. ESRI, Inc.

Ministry of Agriculture, Iraqi Agrometeorological Center, n.d. Iraqi Agrometeorological Center. https://www.agromet.gov.iq/

Najafi, H., Shrestha, P.K., Rakovec, O., Apel, H., Vorogushyn, S., Kumar, R., and Samaniego, L., 2024. High-resolution impact-based early warning system for riverine flooding. Nature Communications, 15(1), 3726. https://doi.org/10.1038/s41467-024-XXXXX

Noma, H. B., and Mohammed, Y. H., 2017. Hydrological Changes in the Marches of Southern Iraq and Their Effect on Development and Environment. ADAB AL-BASRAH, 80, Pp. 334-361. https://un.uobasrah.edu.iq/papers/3106.pdf

Reddy, P.J.R., 2005. A textbook of hydrology. Firewall Media.

Sadana, T., Aerts, J.C., Eilander, D., Merz, B., de Moel, H., Busker, T., and de Bruijn, J., 2025. Validation of the open-source hydrodynamic model SFINCS on historical river floods at the global scale. EGUsphere, 2025, Pp. 1–37. https://doi.org/10.5194/egusphere-2025-XXX

Salami, A.W., Bilewu, S.O., Ibitoye, B.A., and Ayanshola, M.A., 2017. Runoff hydrographs using Snyder and SCS synthetic unit hydrograph methods: A case study of selected rivers in southwest Nigeria. Journal of Ecological Engineering, 18(1). https://doi.org/10.12911/22998993/66258

Salman, Q.M.K., and Hamdan, A.N.A., 2023. Estimation of the curve number for the Lesser Zab watershed using GIS and HEC-GeoHMS. AIP Conference Proceedings, 2775(1), 050007. https://doi.org/10.1063/5.0142XXX

Sayama, T., Yamada, M., Yamakita, A. and Sugawara, Y., 2025. Parameter regionalization of large-scale distributed rainfall–runoff models using a conditional probability method. Progress in Earth and Planetary Science, 12(1), 17. https://doi.org/10.1186/s40645-025-XXXX

Shamsi, U.M., 2008. Arc Hydro: A framework for integrating GIS and hydrology. Journal of Water Management Modeling. https://doi.org/10.14796/JWMM.R228-11

US Army Corps of Engineers, Hydrologic Engineering Center, 2000. HEC-HMS user's manual. Hydrologic Engineering Center.

Yeh, H.F., and Chen, H.Y., 2022. Assessing the long-term hydrologic responses of river catchments in Taiwan using a multiple-component hydrograph approach. Journal of Hydrology, 610, 127916. https://doi.org/10.1016/j.jhydrol.2022.127916

Yousif, Y. T., and Hamdan, A. N., 2026. Flood simulation utilizing HEC-HMS and HEC-RAS. Civil Engineering Journal, 12(1), Pp. 231-251.

Zotou, I., Karamvasis, K., Karathanassi, V. and Tsihrintzis, V.A., 2022. Potential of two SAR-based flood mapping approaches in supporting an integrated 1D/2D HEC-RAS model. Water, 14(24), 4020. https://doi.org/10.3390/w14244020